

2017©IEEE. Personal use of this material is permitted. Permission from IEEE must be obtained for all other uses, in any current or future media, including reprinting/republishing this material for advertising or promotional purposes, creating new collective works, for resale or redistribution to servers or lists, or reuse of any copyrighted component of this work in other works.

LIMB-VIEWING HYPERSPECTRAL IMAGE SIMULATION BASED ON A POLYGONAL EARTH CROSS-SECTION (PEX) MODEL

Alexander Singer-Berk, Steven Richtsmeier and Robert Sundberg

Spectral Sciences, Inc., 4 Fourth Avenue, Burlington, MA 01803-3304

ABSTRACT

This paper will discuss recent improvements made to the Monte Carlo Scene (MCScene) code to enable limb-viewing scenarios and situations where the sun is below the horizon. MCScene is a high fidelity model for full optical spectrum (UV through LWIR) hyperspectral image (HSI) simulation. MCScene provides an accurate, robust, and efficient means to generate HSI scenes for algorithm validation. MCScene utilizes a Direct Simulation Monte Carlo (DSMC) approach for modeling 3D atmospheric radiative transfer (RT). MCScene includes full treatment of molecular absorption and Rayleigh scattering, aerosol absorption and scattering, and multiple scattering and adjacency effects, as well as scattering off spatially inhomogeneous surfaces described by bidirectional reflectance distribution functions (BRDFs). The algorithm models land and ocean surfaces, 3D terrain, 3D surface objects, and effects of realistic finite clouds with surface shadowing. This paper will provide a brief overview of how RT elements are incorporated into the Monte Carlo engine and the recent additional of a polygonal earth cross-section (PEX) method for modeling horizon effects.

Index Terms— Hyperspectral, Multispectral, Simulation, Visible, Infrared

1. INTRODUCTION

Remote hyperspectral and multispectral imagery (HSI and MSI) of the Earth has proven to be highly valuable for numerous applications, including mineral prospecting, and environmental and land use monitoring. The quality of the data products depends critically on the accuracy of the atmospheric compensation, surface reflectance or emissivity/temperature retrieval, detection and identification, and other algorithms. Thus, there is a need for accurate, robust, and efficient means for algorithm validation. For this purpose, high fidelity simulated imagery can provide a practical alternative to field measurements, which are typically expensive, time consuming, and impractical for covering the full range of anticipated atmospheric and surface conditions.

We provide a brief review of the MCScene HSI/MSI image simulation capability [1,2], which is based on a DSMC approach for modeling the 3D radiative transport, and we report on recent improvements in the modeling of long paths through the atmosphere. MCScene can treat land and ocean surfaces, effects of finite clouds [3-5], and other complex spatial effects. The well-known drawback to the DSMC approach is the very

large number of trial “photons” needed to achieve an accurate result, leading to very long computation times. However, recent advances in computing speed combined with convenient and affordable parallel processing systems are overcoming this limitation.

The basic DSMC methodology for the reflective spectral domain is described in Section 2. This section begins with an overview of the model and a discussion of the recently implemented long slant-path approach. Section 3 illustrates this long atmospheric path feature with a variety of simulations, including a limb-viewing sensor scenario, and a simulation with the sun below the horizon.

2. REFLECTIVE SPECTRAL DOMAIN

2.1. Model Overview

MCScene incorporates all optical effects important for solar-illuminated and thermal emission sourced scenes with arbitrary solar illumination and sensor viewing geometries. The optical effects include molecular and aerosol absorption and multiple scattering, surface scattering with material-dependent BRDFs, surface adjacency effects, and multiple scattering and shading by 3D cloud fields. MCScene was originally designed for simulating airborne- or satellite-based sensors looking down onto the earth; the new long path feature discussed in the next subsection allows MCScene to perform simulations for arbitrary sensor geometries, including up-look or limb viewing. As shown in Figure 1, the basic building block of the “MCScene-simulated world” is a cube, nominally 50 km on a side, that encloses a user-definable atmosphere containing molecular species, aerosols, and clouds, and a base representing the ground. The sensor spatial and spectral resolution, its location, and the viewing angle are also specified. The field-of-view (FOV) is an independently gridded region illustrated for a downward viewing scenario in Figure 1.

Surface reflectance properties in a sub-region of the ground are assigned on a pixel-by-pixel basis. For downward viewing simulations, the sensor FOV is typically focused on this pixel region. The pixels can extend to the full MCScene world. Alternatively, the ground that surrounds the reflectance pixels is modeled to be spatially homogeneous, a simplification that generally only affects the regions of the FOV focused near or on the homogeneous region. The reflectance functions for the ground materials are typically represented as Lambertian, however MCScene does include a computationally simple, readily sampled empirical BRDF [6]. More advanced BRDF models can be integrated into MCScene by incorporating their sampling statistics into the model.

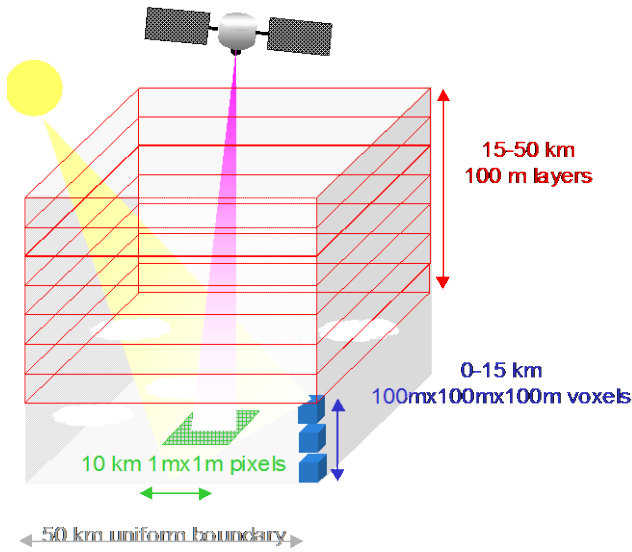


Figure 1. Elements of the scene definition in the simulation model.

Atmospheric information is stored as vertical profiles indexed to ground pixels. The atmosphere below ~15 km altitude is divided into 100 m x 100 m x 100 m voxels, whose footprints cover the full 50 km square world. The atmosphere from 15 to 50 km is modeled by a single uniform profile with 100 m vertically spaced layers and no horizontal variability. The atmospheric profiles specify the altitude dependence of spectral Rayleigh scattering and particulate (aerosol, cloud and rain) extinction and scattering coefficients. The profiles also define densities for molecular species.

The image simulation is performed utilizing a backward DSMC RT technique (the term “backward” Monte Carlo as opposed to “forward” is used to denote tracing of photons backwards along trajectories from the sensor). The major advantages of DSMC over other scattered radiance techniques are its simplicity, accuracy, and versatility, enabling rigorous modeling of complex 3D effects of clouds, shadowing, adjacency, terrain topography, etc. The major drawback of the DSMC technique is that it is computationally intensive. In the current model, the bulk of the computation time is spent sampling distributions and calculating photon path transmittances. These transmittance calculations have been optimized by using a fixed integration path length within altitude regions together with nearest-neighbor extinction coefficient data. This optimization, along with a physics-based *importance sampling* of the distributions influencing photon trajectories and on-the-fly convergence testing, makes the processing efficient enough to enable generation of HSI.

In the backward DSMC method, many photons are launched for each sensor pixel, their trajectories are followed, and their contributions to the apparent reflectance are accumulated to build up the scene at a given spectral channel. Along these trajectories, the photons may be scattered by molecules, aerosols, or clouds, they may be absorbed, or they may reflect from the ground. MODTRAN® [7] generated optical property databases provide the required spectral

scattering and absorption data used in the model. The mathematics of the Monte Carlo sampling algorithms are discussed elsewhere [1]. A given photon may undergo multiple scattering events. A complete data cube is built up by performing the calculations for many different wavelength channels.

The total apparent spectral reflectance is calculated by summing the atmospheric and surface scattering event contributions. The photon position and direction are initialized based on the sensor geometry, and a path optical depth is randomly selected. If the photon scatters within the atmosphere or reflects off the ground, its contribution to the total solar scattered apparent reflectance is summed. The trajectory is terminated if the photon weight drops below a cutoff value or a maximum number of scattering events is reached. Otherwise, a new photon direction is randomly selected from the scattering distribution, and the photon trajectory continued. If the photon exits the solution region, its trajectory is discontinued.

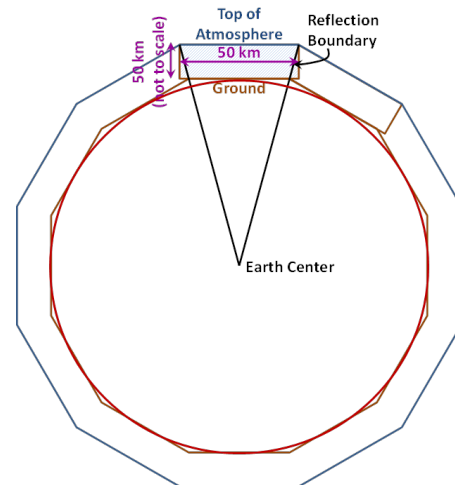


Figure 2. Polygonal earth cross-section model for MCSce.

2.2. Polygonal Earth Cross-section Model

MCSce has recently been extended, MCSceXL, allowing photon trajectories to extend beyond the sides of the nominally 50 km on a side calculation domain shown in Figure 1. The approach for extra-long photon path lengths is illustrated in Figures 2 and 3. Imagine the simulation domain cube sitting on a sphere with the earth’s radius. Reflective boundary cubes are defined whose edges form vertical planes, which, if extended, would pass through the earth center (the proper term for the 3D shapes are right pyramidal frustrums). The cube is filled with the atmosphere, terrain, clouds, and 3D objects as before. Photons are still launched from the sensor and tracked through their trajectories. Now, however, there are no side exits allowed for the photons. If a photon strikes a reflective boundary, it is reflected back into the cube with a revised trajectory, and with the sun moved so its updated position provides consistency with the original trajectory (see Figure 3).

The representation is not as coarse as is depicted in Figure 2. The earth-centered angle $\Delta\theta$ measures $<0.45^\circ$, so the true

cross section contains over 800 trapezoids, not just the 12 implied by the figure. Re-using the calculation domain means that we are not required to carry around a terrain and atmosphere representation spanning hundreds or possibly thousands of kilometers. We could also account for spherical refraction effects at reflection boundaries, though this is not yet supported. However, the code has been generalized to allow the sensor to look away from the ground, enabling limb viewing or up-looking views.

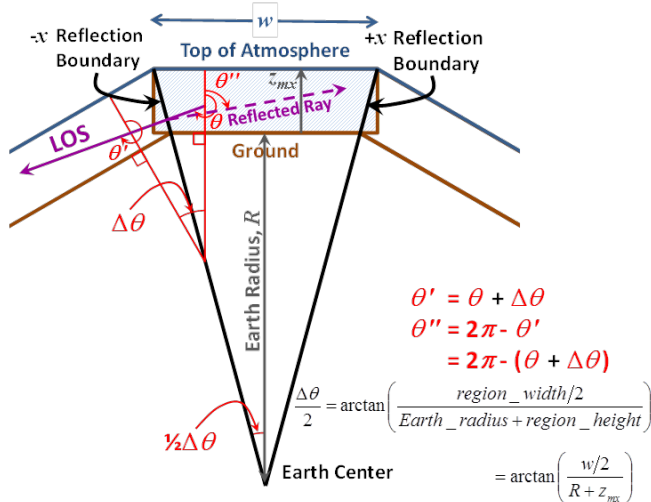


Figure 3. Calculation of reflected trajectories for MCSceXL, the new, extra-long trajectory version of MCSce.

2.3. Image Simulation

To illustrate the new long-path simulation feature, a scene was constructed based on surface reflectance spectra retrieved from Landsat imagery taken over Woomera, South Australia. The data was atmospherically corrected using the FLAASH[®] code [8]. RGB rendering of the terrain imagery is shown in Figure 4. The terrain image contains 2001 × 2001 pixels, and the pixel side length is 25 m. A cirrus cloud field has been embedded in the image with a 8 km base altitude. The cloud field was extracted from Landsat imagery and has a maximum optical depth of 2 at 550 nm. The atmosphere profiles used in the simulation are taken from MODTRAN's mid-latitude summer (MLS) model with a rural aerosol. The simulated color composite imagery (0.47, 0.54, and 0.65 μm) for a limb-viewing sensor at 6.5 km altitude looking West, Southwest, and South are shown in Figure 5. The solar zenith angle for these simulations was 30°, with the sun due East. The horizontally centered sensor FOV was 102° × 102°.

Two additional long-path limb-view simulation scenarios are illustrated by the simulations shown in Figure 6. The left side of the figure shows color composite imagery (R, G, B = 0.65, 0.54, and 0.47 μm) for an observer at 2 km altitude looking west as the sun has set 2° below the horizon. The sensor FOV was 8.4° × 34°. The image on the right side of Figure 6 is for an observer looking west with the sun 5° above the horizon but behind an optically opaque cumulus cloud. The

cumulus cloud geometry and optical opacity were derived from Landsat imagery [9]. The cloud base altitude was 1 km, and the sensor was placed at a distance of 10 km from the cloud at an altitude of 1 km. The sensor FOV was 34° × 51°. As before, the atmosphere for both simulations was the MLS model with rural aerosols.



Figure 4. Landsat reflectance imagery showing terrain in Southern Australia used in long-path simulation.

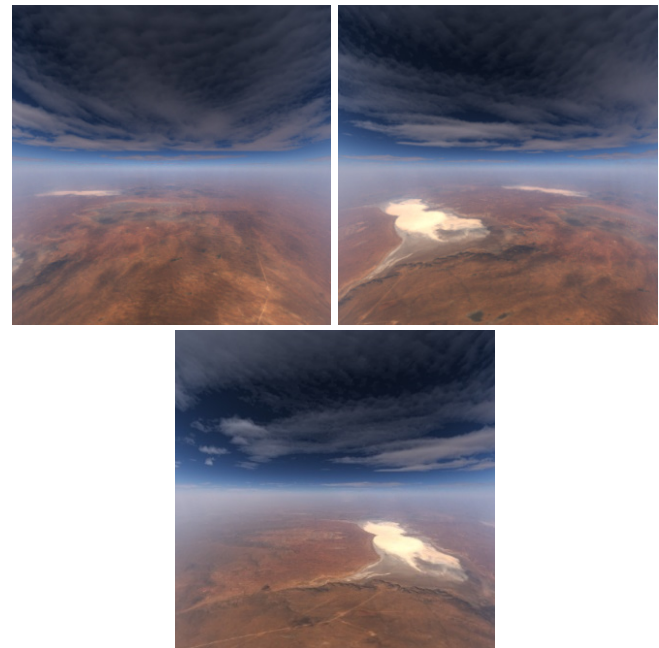


Figure 5. MCSce color composite imagery for a sensor at 6.5 km altitude looking West (top left), Southwest (top right), and South (bottom).

Most recently, Steven Richtsmeier collaborating with David K. Lynch and David S.P. Dearborn to study the structure and optics of the antisolar twilight sky [10, 11]. MCSce

calculations were used to help understand observations of the colors of clear sky opposite the sun when the sun is a few degrees below the horizon. The redish Belt of Venus is clearly evident above the dark blue band. The video image was recorded in Malibu, CA at 7:04:25 PST on 31 Dec 2015. The MCScene calculation was run using the MLS atmosphere with clear sky conditions (no clouds or aerosols).

3. CONCLUSIONS AND FUTURE WORK

The MCScene model has been upgraded to allow for long paths through the atmosphere. This new feature allows for accurate simulations for scenarios which include limb-viewing sensors and sun locations below the horizon. The current capabilities of the simulation code are unique and state-of-the-art, and are highlighted by the use of a rigorous radiative transport approach, a full 3D treatment of the atmosphere, including finite 3D cloud fields, surface BRDFs, and a faceted surface description incorporating surface elevation and 3D objects.

4. ACKNOWLEDGMENT

The authors wish to acknowledge Spectral Sciences, Inc. for support under an internal research and development grant.

5. REFERENCES

- [1] S. Richtsmeier, A. Berk, S.M. Adler-Golden, and L.S. Bernstein, "A 3D Radiative-Transfer Hyperspectral Image Simulator for Algorithm Validation," *Proceedings of ISSSR 2001*, Quebec City, Canada, June 2001.
- [2] W. Pereira, S. Richtsmeier, S. Carr, S. Kharabash, and A. Brady, "A Comparison of MCScene and CameoSim Simulations of a Real Scene," *Proceedings of IEEE 2014, Whispers 2014 Conference*, Lausanne, Switzerland, June 2014.
- [3] R.L. Sundberg and S. Richtsmeier, "Reflectance Retrieval in the Presence of Optically Opaque Broken Clouds," in *IEEE GRSS Workshop on Hyperspectral Image and Signal Processing: Evolution in Remote Sensing (WHISPERS)*, 6th Workshop, 2014.
- [4] S. Richtsmeier and R.L. Sundberg, "Full Spectrum Cloud Scene Simulation," *IEEE International Geoscience & Remote Sensing Symposium*, Melbourne, Australia, July 21-26, 2013.
- [5] S. Richtsmeier, A. Singer-Berk, and R.L. Sundberg, "Full Spectrum Cloudy Scene Simulation," *SPIE Proceedings, Algorithms and Technologies for Multispectral, Hyperspectral, and Ultraspectral Imagery XVI*, Vol. 7695, 2010.
- [6] C.L. Walthall, J.M. Norman, J.M. Wes, G. Campbell, and B.L. Blad, "Simple Equation to Approximate the Bidirectional Reflectance from Vegetation Canopies and Bare Soil Surfaces," *Appl. Optics* 24:383-387 1985.
- [7] A. Berk and F. Hawes, "Validation of MODTRAN[®]6 and its Line-By-Line Algorithm," submitted for publication to *J. Quant. Spectrosc. Radiat. Transfer*, October, 2016.
- [8] S.M. Adler-Golden, M.W. Matthew, L.S. Bernstein, R.Y. Levine, A. Berk, S.C. Richtsmeier, P.K. Acharya, G.P. Anderson, G. Felde, J. Gardner, M. Hoke, L.S. Jeong, B. Pukall, J. Mello, A.

Ratkowski, and H.-H. Burke,, "Atmospheric Correction for Short-wave Spectral Imagery based on MODTRAN4," *SPIE Proceeding, Imaging Spectrometry V*, Vol. 3753, 1999.

[9] S.M. Adler-Golden, S. Richtsmeier, R. Panfili, X. Jin, J.W. Duff, J.G. Shanks, and A. Dudkin, "Next Generation Terrain and Cloud Background Models for System Studies," Spectral Sciences, Inc., Report No. SSI-TR-635, Phase II Final Report, prepared for United States Army Space and Missile Defense Command under Contract No. W9113M-10-C-0081, 2012.

[10] D.K. Lynch, D.S.P. Dearborn and S.C. Richtsmeier, "Antitwilight I: Structure and Optics," *Appl. Opt.* 56, G156-G168 (2017).

[11] S. Richtsmeier, D.K. Lynch and D.S.P. Dearborn, "Antitwilight II: Monte Carlo studies," *Appl. Opt.* 56, G169-G178 (2017).

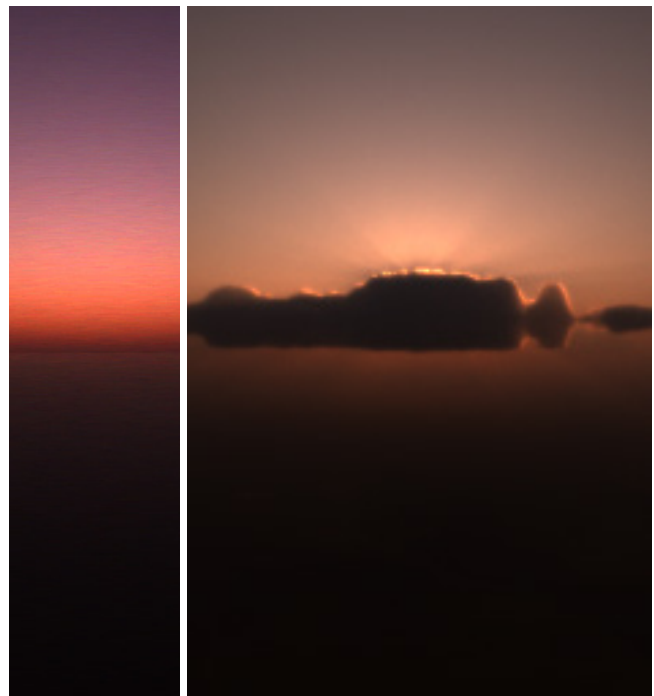


Figure 6. Simulations with the sun 2° below the horizon (left), and 5° above the horizon, behind cumulus clouds (right).



Figure 7. An RGB comparison of the anti-solar point with the sun 1° below the (opposite) horizon. A video image on the left was taken in Malibu, CA at 7:04:25 PST on 31 Dec 2015. The MCScene simulation is shown on the right.